THE JOURNAL OF BIOLOGICAL CHEMISTRY
Vol. 274, No. 34, Issue of August 20, pp. 23820–23827, 1999

Printed in U.S.A.

Heterologous Expression of the Vanadium-containing Chloroperoxidase from *Curvularia inaequalis* in *Saccharomyces cerevisiae* and Site-directed Mutagenesis of the Active Site Residues His^{496}, Lys^{353}, Arg^{360}, and Arg^{490}*

(Received for publication, March 5, 1999, and in revised form, June 2, 1999)

Wieger Hemrika‡, Rokus Renirie‡, Sandra Macedo-Ribeiro§, Albrecht Messerschmidt§, and Ron Wever‡¶

From the ‡E. C. Slater Institute, Faculty of Chemistry, University of Amsterdam, Plantage Muidergracht 12, 1018 TV Amsterdam, The Netherlands and the §Max-Planck Institut fur Biochemie, Abteilung Strukturforsung, Am Klopferspitz 18 A, D-82152 Martinsried, Germany

The vanadium-containing chloroperoxidase from the fungus *Curvularia inaequalis* is heterologously expressed to high levels in the yeast *Saccharomyces cerevisiae*. Characterization of the recombinant enzyme reveals that this behaves very similar to the native chloroperoxidase. Site-directed mutagenesis is performed on four highly conserved active site residues to examine their role in catalysis. When the vanadate-binding residue His^{496} is changed into an alanine, the mutant enzyme loses the ability to bind vanadate covalently resulting in an inactive enzyme. The negative charges on the vanadate oxygens are compensated by hydrogen bonds with the residues Arg^{360}, Arg^{490}, and Lys^{353}. When these residues are changed into alanines the mutant enzymes lose the ability to effectively oxidize chloride but can still function as bromoperoxidases. A general mechanism for haloperoxidase catalysis is proposed that also correlates the kinetic properties of the mutants with the charge and the hydrogen-bonding network in the vanadate-binding site.

Haloperoxidases are enzymes catalyzing the two-electron oxidation of a halide (X^-) to the corresponding hypohalous acid (HOX) according to Equation 1.

$$H_2O_2 + H^+ + X^- \rightarrow H_2O + HOX \qquad \text{(Eq. 1)}$$

This hypohalous acid may further react with a broad range of nucleophilic acceptors to form a diversity of halogenated compounds. The haloperoxidases are named after the most electronegative halide they are able to oxidize, implying that a chloroperoxidase can oxidize chloride, bromide, and iodide, whereas a bromoperoxidase can oxidize bromide and iodide.

The vanadium haloperoxidases (VHPO)[1] form one of the three groups of haloperoxidases that are currently known. These enzymes were first discovered in marine macroalgae (seaweeds) (1–3) but are also shown to be present in fungi (4) and in a lichen (5). The most studied fungal vanadium haloperoxidase is the vanadium chloroperoxidase (VCPO) from the plant pathogenic fungus *Curvularia inaequalis* (6–13). This enzyme is found associated with the fungal hyphae (13) but can also be isolated from the growth medium of the fungus. When vanadate is absent from the growth medium of the fungus, the enzyme is present in its inactive apo form. This apoenzyme can easily be activated by the addition of vanadate (6) indicating that auxiliary protein factors are not essential for incorporation of the cofactor.

The gene encoding the *C. inaequalis* VCPO has been cloned and sequenced (10). The gene codes for a protein of 609 amino acids with a calculated molecular mass of 67,488 Da. Determination of the crystal structure of this enzyme (11) revealed a molecule with an overall cylindrical shape measuring about 80×50 Å. The secondary structure is mainly α-helical with two four-helix bundles as main structural motifs of the secondary structure. The active site of the enzyme is located on top of the second four-helix bundle. The vanadium ion, which is present in its highest oxidation state (5^+) as hydrogen vanadate (HVO_4^{2-}), is coordinated to the protein in a trigonal bipyramidal fashion with three oxygen atoms in the equatorial plane (Fig. 1). A covalent bond is formed at one apical position with atom $N^{\epsilon 2}$ of His^{496}, and a hydroxide group is present at the other apical position where it forms a hydrogen bond with $N^{\delta 1}$ of His^{404} (14). The negative charges of the equatorial vanadate oxygens are compensated by hydrogen bonds to surrounding hydrophilic or positively charged protein groups (Lys^{353}, Arg^{360}, Ser^{402}, Gly^{403}, and Arg^{490}).

Analysis of the peroxide form of the enzyme reveals a distorted tetragonal coordination geometry (14). The apical hydroxide group has been released, and His^{404} is no longer hydrogen-bonded to any oxygen function of the vanadate. The peroxide binds side-on in the equatorial plane. One of the peroxide oxygens is hydrogen-bonded to Lys^{353} and to the amide nitrogen of Gly^{403} a residue that also makes a hydrogen bond to the other oxygen of the peroxide. Arg^{360} and Arg^{490} remain hydrogen-bonded to the same oxygens as in the native structure.

The active site residues are conserved in three short domains in other VHPOs and most interestingly in several families of acid phosphatases that were considered unrelated (11, 15, 16). Therefore we proposed that these enzymes have structurally very similar active sites. The homologous acid phosphatases contain important enzymes such glucose-6-phosphatase (17–

* This work was supported by the Council of Chemical Sciences of the Netherlands Organization for Scientific Research and was made possible by financial support from the Netherlands Organization for Scientific Research, the Netherlands Technology Foundation, and the Netherlands Association of Biotechnology Centers. The costs of publication of this article were defrayed in part by the payment of page charges. This article must therefore be hereby marked "*advertisement*" in accordance with 18 U.S.C. Section 1734 solely to indicate this fact.

¶ To whom correspondence and reprint requests should be addressed. Tel.: 31 20 5255058; Fax: 31 20 5255124; E-mail: a311rw@chem.uva.nl.

[1] The abbreviations used are: VHPO, vanadium haloperoxidase; VCPO, vanadium-containing chloroperoxidase; rVCPO, recombinant enzyme VCPO; VBPO, vanadium bromoperoxidase; kb, kilobase pair(s); PAGE, polyacrylamide gel electrophoresis.

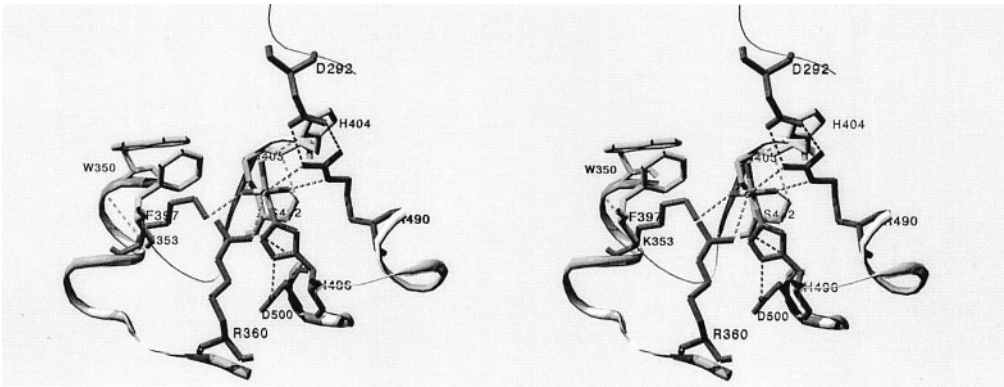

FIG. 1. **Stereoview of the native VCPO active site, adapted from Ref. 14 and created with Swiss-PDB-Viewer (45) and POV-Ray 3.0 software**.

19), an enzyme that plays a key role in gluconeogenesis and glucose homeostasis (20), and the phosphatidic acid phosphatases (21–23), which are enzymes thought to be involved in signal transduction.

Although spectroscopic and kinetic studies have revealed many details about the metal-binding site and the reaction mechanisms of both the VBPOs and the VCPOs, the precise role of the active site residues has remained elusive. In trying to gain information about such roles we have created heterologous expression systems in which the *C. inaequalis VCPO* gene is expressed in *Escherichia coli* (24) or in the yeast *Saccharomyces cerevisiae*. Although the bacterial expression system was shown to produce recombinant enzyme (rVCPO) that could be activated by adding vanadate, the amount of enzyme that could be isolated from this system was very low, hampering in depth analysis of the recombinant enzyme (24).

Here we describe a yeast recombinant expression system that enables us to isolate large amounts of recombinant (apo) enzyme. Determination of the kinetic parameters of this recombinant enzyme shows that these are essentially identical to those of the native enzyme. This *S. cerevisiae* expression system enables us to create site-directed mutants for rVCPO.

Binding and coordination of the vanadate cofactor in the VCPO active site are expected to be essential for enzymic activity. As a first approach in the analysis of the roles of the active site residues in catalysis, we have examined the effects of mutating the basic residues His^{496}, Lys^{353}, Arg^{360}, and Arg^{490} into alanines. We show that His^{496} is essential for VCPO catalysis and that the K353A, R360A, and R490A mutations basically convert the mutant enzymes into VBPOs. Finally the (gradual) effects of the mutations of residues Lys^{353}, Arg^{360} and Arg^{490} are discussed in a proposed general mechanism for VHPO catalysis.

EXPERIMENTAL PROCEDURES

Strains and Media—E. coli strains HB101 and JM109 were used for the propagation of recombinant DNA constructs. Strains ES1301 mutS (Promega) or Epicurian XL1-blue (Stratagene) were used for the propagation and selection of plasmids after site-directed mutagenesis. *E. coli* transformants were grown in YT medium (1% w/v yeast extract, 1% w/v casein lysate, and 0.5% w/v NaCl) containing 100 μg of ampicillin for normal transformation or 10 μg/ml tetracycline after (Altered sites®) site-directed mutagenesis.

S. cerevisiae strain BJ1991 (*Matα, leu2, trp1, ura3-251, prb1-1122, pep4-3*) was used as the host of the expression plasmids carrying the wild type or the mutant *C. inaequalis VCPO* genes. Transformation of yeast was performed according to Ref. 25. Transformants were selected on minimal medium containing 0.67% (w/v) yeast nitrogen base (Difco), 2% (w/v) glucose, 2% (w/v) agar supplemented with tryptophan (20 μg/ml) and leucine (50 μg/ml). Inducible expression of rVCPO was checked by growing yeast transformants in rich medium containing 1% (w/v) yeast extract, 1% (w/v) casein lysate, 2% (w/v) agar, and either 2% galactose (induction) or 2% glucose (repression).

Construction of the rVCPO Expression Vector—Fig. 2 shows a schematic representation of the DNA fragments and the plasmids used to construct the recombinant expression vector.

The 0.8-kb *Eco*RI-*Bam*HI fragment containing the inducible *S. cerevisiae Gal1* promoter (26, 27) was cloned into *Bam*HI-*Eco*RI-digested Yeplac195 (a multi-copy yeast shuttle vector) (28) giving plasmid pTNT2. The *Eco*RI site of pTNT2 was removed by digestion with *Eco*RI, filling the ends with Klenow polymerase and religation, giving pTNT12.

The *C. inaequalis VCPO* gene was present in pUC18 as a 2.5-kb *Pst*I-*Eco*RI genomic DNA fragment containing the 1.1-kb 5′-half of the *VCPO* gene or as a 0.8-kb *Eco*RI-PvUII genomic DNA fragment containing the 3′-half of the gene, respectively (10).

A *Bam*HI restriction site was created, at position −44 with respect to the *VCPO* start codon, by polymerase chain reaction using *Tac* polymerase (Promega) and as primers the M13/pUC 22-mer reverse sequence primer and primer WH1-Bam, 5′-GAGAGAGGATCCACTCACTACT-TACAATCACAC-3′. After polymerase chain reaction amplification this fragment was isolated and digested with *Bam*HI and *Eco*RI.

The *Bam*HI site present in pUC18 containing the 3′ end of the *VCPO* gene was destroyed by *Bam*HI digestion, filling of the ends, and religation, giving pTNT13. Digestion with *Eco*RI and *Xba*I liberated the 3′ *VCPO* fragment. A three-point ligation was used to ligate the 5′ *Bam*HI-*VCPO-Eco*RI fragment and the 3′ *Eco*RI-*VCPO-Xba*I fragment into pTNT12 digested with *Bam*HI and *Xba*I. This resulted in pTNT14, the inducible yeast expression vector. Plasmid pTNT14 was transformed to yeast, and transformants were checked for VHPO activity using the *o*–dianisidine or the phenol red assay.

Isolation of rVCPO—Yeast cells shown to express rVCPO were inoculated into starter cultures containing 0.67% yeast nitrogen base without amino acids (YNB-WO Difco), 2% (w/v) glucose, and 20 μg/ml (w/v) uracil and grown until the end of the log phase. Starter cultures were diluted 1:10 in 1% (w/v) yeast extract (Difco), 1% casein hydrolysate (Difco), and 1% (w/v) glucose and grown until the end of the log phase. The cultures were induced by the addition of galactose to a final concentration of 4% (w/v) and allowed to grow for another 2 days.

The yeast cells were harvested by centrifugation (5 min at 3000 × *g*) and resuspended to 1 g/ml in 50 mM Tris/HCl, pH 8.1. An equal volume of acid-washed glass beads (425–600 μm, Sigma) was added, and the yeast cells were broken using an ice water-cooled bead beater (Biospec) for 5 × 2 min. The suspension was collected, and the glass beads were washed with 2 volumes of 50 mM Tris/HCl, pH 8.1. After centrifugation (15 min at 5000 × *g*) an equal volume of isopropyl alcohol was added to the supernatant to precipitate nucleic acids. After centrifugation (20 min at 13,000 × *g*), the clear supernatant was applied to a DEAE-Sephacel column (Amersham Pharmacia Biotech) (0.2 ml slurry/ml supernatant) equilibrated with 50 mM Tris/HCl, pH 8.1. After washing of the column with 2 volumes of 50 mM Tris/HCl, pH 8.1, and 2 volumes of 0.1 M NaCl in 50 mM Tris/HCl, pH 8.1, the enzyme was eluted with 0.6 M NaCl in 50 mM Tris/HCl, pH 8.1. Upon dialysis against 20 mM piperazine HCl, pH 5.4, a final purification step was performed using a Poros 20 HQ anion exchange column (Perspective Biosystems). The enzyme was eluted with a linear gradient of 0.1 to 1.0 M NaCl in 20 mM piperazine HCl, pH 5.4. Finally the pure apoenzyme was dialyzed against 50 mM Tris acetate, pH 8.1, or against 100 μM orthovanadate in 50 mM Tris acetate, pH 8.1, followed by 50 mM Tris acetate, pH 8.1, to obtain the reconstituted holoenzyme.

Production of the Mutant Enzymes—rVCPO mutants were produced using either the Altered Sites II (Promega) or the Quickchange Site-directed Mutagenesis Kit (Stratagene). For the H496A and R490A

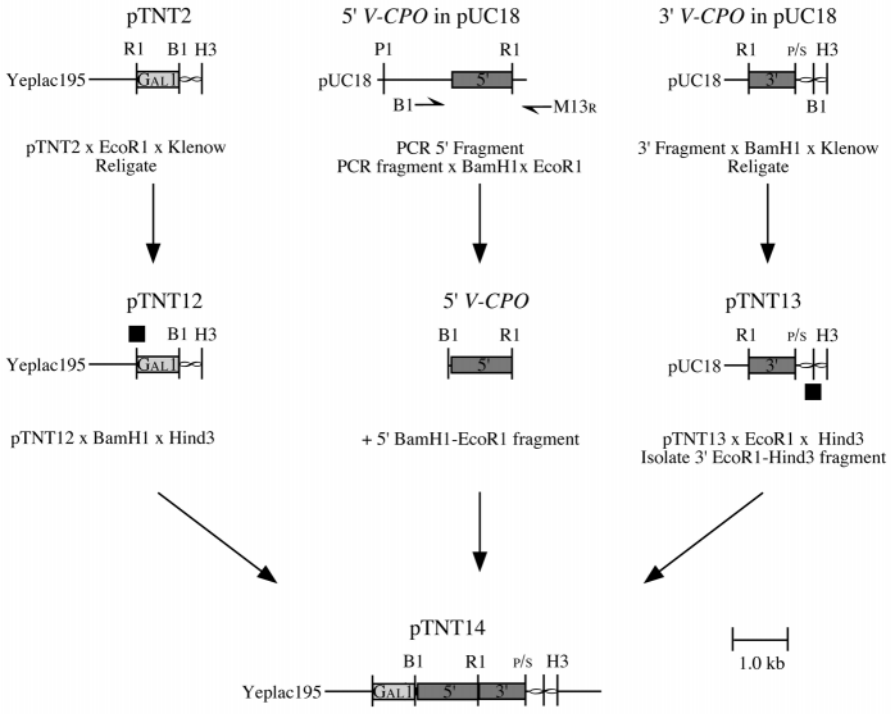

FIG. 2. **Plasmids and fragments used for the construction of the rVCPO expression vector.** See text for details of the construction. The endonuclease sites used are indicated as follows: *R1, Eco*RI; *B1, Bam*HI; *P1, Pst*I; *H3, Hin*dIII; ∞, pUC polylinker; *P/S,* disrupted *Sma*I site which is the result of the insertion of the 3′ VCPO *Eco*RI-*Pvu*II fragment into pUC18 digested with *Eco*RI and *Sma*I (10); ■, disrupted *Eco*RI or *Bam*HI site.

mutants the 0.8-kb 3′ *Eco*RI-*Hin*dIII fragment from pTNT14 was ligated into pAlter1 (Promega) digested with the same enzymes. Mutagenesis was performed according to the manufacturer's protocol using the primers 1-(H496A) 5′-CCTCGGTGTCGCCTGGCGTTTCGAT-3′ and 2-(R490A) 5′-ACGCCATTTCGGCCATCTTCCTCGG-3′, and after mutagenesis the plasmids were sequenced and fragments carrying the desired mutations were ligated back into pTNT14 digested with *Eco*RI and *Hin*dIII. Mutants R360A and K353A were made directly in pTNT14 according to the Quickchange protocol using the primers 3-(R360A) 5′-TTCGAATTCTGGGCCCCACTATCTGGT-3′ and the complementary primer 4-(R360Acomp.) 5′-ACCAGATAGTGGGGCCCAGAATTCGAA-3′ or 5-(K353A) 5′-TCCTGGAAGGAGGCCTGGGAGTTCGAA-3′ and 6-(K353Acomp.) 5′-TTCGAACTCCCAGGCCTCCTTCCAGGA-3′. After checking for the desired mutation by manual sequencing using the T7 Sequencing kit (Amersham Pharmacia Biotech) the mutated pTNT14 derivatives were transformed to yeast. Mutant enzymes were isolated as described for rVCPO.

SDS-PAGE Analysis—SDS-polyacrylamide gel electrophoresis was carried out using 7% gels according to Laemmli (29) under either denaturating conditions (boiling of sample for 5 min in the presence of SDS and β-mercaptoethanol) or native conditions (in the presence of SDS but without β-mercaptoethanol and boiling). The presence of SDS in native SDS-PAGE analysis does not affect enzymic activity (10, 13) and thus the presence of active enzyme in the gel can be assessed by soaking it in 1 mM *o*-dianisidine, 50 mM KBr, 1 mM H_2O_2, 100 μM orthovanadate in 50 mM sodium acetate, pH 5. Denatured samples were observed using Coomassie Brilliant Blue R-250.

Enzyme Activity Assays—VHPO activity can be qualitatively tested using the phenol red assay by incubating aliquots of cells or (partly) purified enzyme in 100 mM phenol red, 50 mM sodium citrate, pH 5, 100 μM orthovanadate, 50 mM KBr, and 10 mM H_2O_2.

VCPO activity was measured quantitatively by following the chlorination/bromination of monochlorodimedone ($\epsilon = 20.2\ mM^{-1}\cdot cm^{-1}$ at 290 nm) to dichlorodimedone ($\epsilon = 0.1\ mM^{-1}\cdot cm^{-1}$ at 290 nm) in 50 mM sodium citrate/citric acid buffer adjusted to the desired pH and using the appropriate concentrations of the substrates chloride or bromide and H_2O_2 in the presence of 100 μM orthovanadate using Popspec software on an Atari 1040ST computer coupled to a single beam Zeiss spectrophotometer via the Poptronics 4-channel A/D converter.

Miscellaneous—Protein concentrations were determined according to Bradford (30). Published procedures were used for DNA manipulations (31). Restriction and other enzymes used in DNA manipulation were purchased from Roche Molecuar Biochemicals and Promega and used as recommended by the manufacturers. Radioactive chemicals were obtained from Amersham Pharmacia Biotech. All other chemicals were of the highest purity available.

RESULTS

Expression of the C. inaequalis VCPO in S. cerevisiae—Since the VCPO of *C. inaequalis* and other hyphomycetes can be isolated from the growth media of these fungi (4), these enzymes are considered to be secretion proteins. Analysis of the predicted amino acid sequence and of the crystal structure of the *C. inaequalis* VCPO, however, did not show the cleavable N-terminal signal sequence that usually directs eukaryotic secretion proteins to the endoplasmic reticulum (10). This feature, together with the absence of post-translational modification steps like the formation of disulfide bridges and *N*-linked glycosylation, suggested the presence of an alternative secretion route for the fungal VCPOs (10). To investigate whether such an alternative route would also be taken when the *C. inaequalis* enzyme was expressed in *S. cerevisiae,* we decided to clone the *VCPO* gene into our yeast expression vector without fusing it to a yeast signal sequence, such as that of the yeast mating type α-factor (32).

Yeast colonies transformed with the pTNT14 expression vector (Fig. 2), as indicated by their Ura^+ phenotype, were streaked on plates containing rich growth medium supplied with either glucose or galactose. After 2 days of growth, cells from the glucose and the galactose plates were separately resuspended in 200 μl of 100 μM orthovanadate in 50 mM Tris/HCl, pH 8.1, spotted on nitrocellulose filters, and incubated in an *o*-dianisidine assay mixture. After several minutes a clear color formation could be observed on spots derived from galactose-grown cells but not on those derived from glucose-grown cells, indicating the presence of a galactose-inducible expression system for rVCPO in yeast. Subsequently, liquid cultures were grown from yeast cells shown to express the rVCPO. Activity as measured in these cultures, however, proved to be associated with the yeast cells and could only be detected to the full level after disruption of the cells, indicating that the rVCPO is not secreted by yeast but remains internal.

In order to obtain a yeast system in which the rVCPO is secreted into the growth medium, we have also made an expression construct in which the *VCPO* gene is fused in frame to the yeast α-factor secretion signal. Surprisingly, no stable ex-

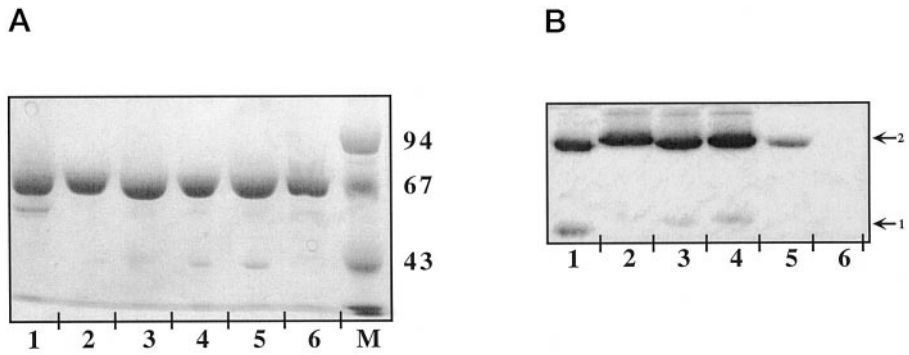

FIG. 3. **SDS-PAGE analysis of VCPO proteins isolated from *C. inaequalis* or yeast (recombinant protein).** 3-μg samples of purified VCPO proteins were separated on 7% SDS-polyacrylamide gels under denaturing conditions (*A*) or native conditions in the absence of β-mercaptoethanol and without boiling (*B*). The proteins are visualized with Coomassie Brilliant Blue (*A*) or by activity staining (*B*). *Lanes 1*, native VCPO from *C. inaequalis*; *lanes 2*, rVCPO; *lanes 3*, mutant R360A; *lanes 4*, mutant R490A; *lanes 5*, mutant K353A; *lanes 6*, mutant H496A; *lane M*, molecular weight marker. *B, arrow 1*, monomeric form of the enzyme; *arrow 2*, high molecular weight aggregate of the enzyme.

pression of the rVCPO could be obtained with this system. This feature was not further investigated since using the internal expression system under optimized growth and isolation procedures (as described under "Experimental Procedures"), we are now able to isolate approximately 100 mg of pure (apo) rVCPO from 1 liter of yeast culture.

Characterization of rVCPO—Apo-rVCPO as isolated from the yeast expression system can, like the native protein as isolated from *C. inaequalis*, easily be activated by incubating the apoenzyme with 100 μM orthovanadate in 50 mM Tris/SO_4, pH 8.1. Furthermore, addition of 100 μM orthovanadate to enzyme activity assay mixtures results in a very rapid activation of the apoenzyme. Fig. 3 shows the results of an SDS-PAGE experiments in which 3-μg samples of purified VCPO were run under either denaturing (Fig. 3*A*) or native (Fig. 3*B*) conditions. Fig. 3*A* shows that the native VCPO (*lane 1*) and the rVCPO (*lane 2*) both run as a single 67-kDa band. It was shown (10) that VCPO remains active in SDS-PAGE gels when β-mercaptoethanol is omitted from the sample buffer, and the samples are not boiled prior to loading. Fig. 3*B, lanes 1* and *2,* shows that, although the monomeric form of the enzymes is also visible, under these conditions both the native and the recombinant CPO run mainly as higher molecular weight aggregates that can be stained for activity.

EPR spectra were taken to characterize further the rVCPO. After reduction of the sample with dithionite, the typical vanadyl spectrum, as already observed for the native VCPO (6) and several VBPOs (33, 34), was obtained (results not shown).

Determination of the rate of chloride oxidation by rVCPO as a function of pH by spectrophotometrically following the chlorination of monochlorodimedon revealed an optimum around pH 5 and a maximal value of k_{cat} of 26 s^{-1}. Furthermore, at this optimal pH the K_m values for H_2O_2 and Cl^- were determined to be 40 μM and 0.9 mM, respectively. The specificity constant calculated from our data for chloride and H_2O_2 are $2.9 \cdot 10^4$ M^{-1} s^{-1} and $6.5 \cdot 10^5$ M^{-1} s^{-1}, respectively. These kinetic parameters are very similar to those reported for the native VCPO (k_{cat} of 23 s^{-1}, K_m H_2O_2 10 μM and K_m Cl^- 0.9 mM) (6, 8).

The x-ray crystal structure of the apo-rVCPO and its reconstituted holo form have been determined very recently (35). It is reported that the overall structure of the rVCPO is nearly identical to that of the native VCPO, which holds particularly for the vanadate-binding site (35). These results confirm that the recombinant enzyme is very similar to the native one. We therefore decided to use this rVCPO as the wild type control in the experiments describing the parameters of the mutant enzymes.

Kinetic Properties of rVCPO and the Mutants—Fig. 3, *A* and *B, lanes 3–6*, shows the purified mutant enzymes run on SDS-PAGE and stained with Coomassie Brilliant Blue for protein identification (Fig. 3*A*) or with *o*-dianisidine to determine activity (Fig. 3*B*). It can be seen in Fig. 3*A* that all mutant proteins run similarly to the native VCPO and the rVCPO. Fig. 3*B, lanes 3–5,* shows that mutants R490A, R360A, and K353A, respectively, retain (bromo) peroxidase activity with that of mutant K353A being very little (*lane 5*). Mutant H496A (Fig. 3*B*, *lane 6*) shows no activity at all. However, when the activity stained gel is subsequently incubated with Coomassie Brilliant Blue, also in *lane 6* a protein band is visible running at the same height as those in *lanes 1–5* of Fig. 3*B* (results not shown).

The results obtained with the non-denaturing SDS-PAGE analysis indicate that the overall structure of the mutant proteins is similar to that of the native VCPO and the rVCPO. This is confirmed by the crystal structures of the mutants that have very recently been analyzed (35). From the mutants studied here, x-ray crystal structures are obtained for mutants H496A and R360A. The crystal structure analysis indicates that the vanadate-binding pocket forms a very rigid frame, stabilizing oxyanion binding. Furthermore, the empty spaces left by the replacement of the large side chains by an alanine are usually occupied by new solvent molecules, which partially replace the hydrogen bonding interactions to the vanadate (35).

A kinetic analysis of the rVCPO and the mutant enzymes was started to evaluate importance of these active site residues in catalysis. It is conceivable that the mutations also affect the affinity of the apoenzyme for the cofactor. This was not investigated, but to compensate for such potential effects the kinetic experiments were performed in the presence of excess (100 μM) orthovanadate.

When the activity of the rVCPO and the mutants was measured with chloride as a substrate it was found that, as expected, mutant H496A was inactive, but also mutants R490A and K353A showed very low chloroperoxidase activity. When the rate of the chlorination reaction was measured as a function of chloride concentration for mutants R490A and K353A, V_{max} conditions were not reached even in the presence of 1 M Cl^-. Thus we were not able to determine the K_m for chloride for these mutants. Furthermore, activity remained less than 1.5% of that of the rVCPO. R360A is the only mutant showing appreciable chloroperoxidase activity although with a much higher K_m for Cl^- (19 mM) and a reaction rate at saturating chloride concentrations which is only 14% that of the rVCPO.

Mutants R490A and K353A have lost the ability to oxidize chloride, but *lanes 4* and *5* of Fig. 3 indicate that these mutants are still able to oxidize bromide; therefore, we decided to determine bromoperoxidase activity in order to characterize further the changes in the kinetic properties of the mutants.

It has recently been shown (36) that the native VCPO has a very high affinity for bromide (K_m 9 μM at pH 5) and that strong substrate inhibition by bromide already occurs at concentrations higher than 0.5 mM. In order to establish the dependence of enzyme activity on pH we therefore measured monochlorodimedon bromination at several pH values at low concentrations of the substrates H_2O_2 and Br^- (0.5 and 0.1 mM, respec-

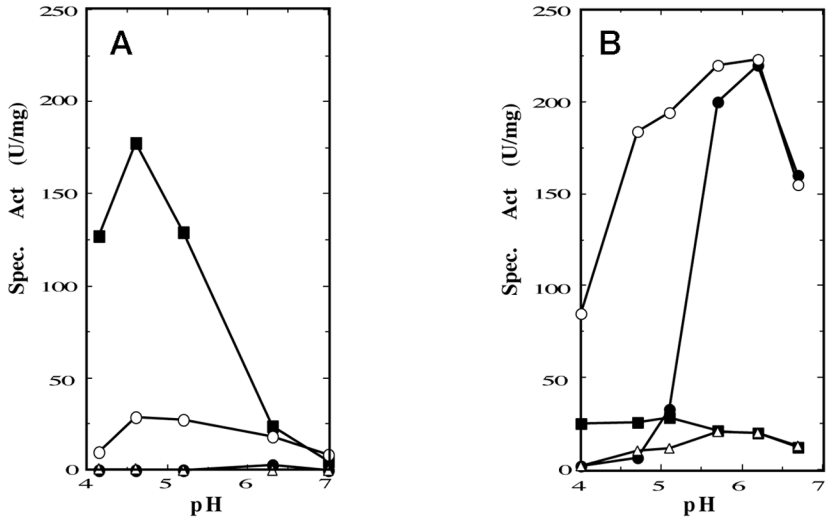

FIG. 4. **Bromoperoxidase activity of rVCPO and mutants R360A, R490A, and K353A as a function of pH.** *A*, 0.5 mM H_2O_2 and 0.1 mM Br^-. *B*, 40 mM H_2O_2 and 20 mM Br^-, all reactions were carried in the presence of 100 μM vanadate. The reaction rates were determined in duplicate. ■, rVCPO; ○, R360A; ●, R490A; △, K353A.

tively). The results of these measurements are depicted in Fig. 4*A*. For the rVCPO optimal bromoperoxidase activity (about 200 s^{-1}) is found at pH 4.6, which is in accordance with the values reported previously (36). As observed for chloride oxidation, mutant R360A is the only mutant showing appreciable bromoperoxidase activity (16% of that of the rVCPO at pH 4.6). Mutants R490A and K353A show at pH 4.6 only 0.3 and 1.6% of wild type activity, respectively. However, the results obtained with the gels stained for bromoperoxidase activity (Fig. 3*B*) already indicated that mutants R490A and K353A possess significant bromoperoxidase activity at higher bromide concentrations. Therefore, we also measured the specific activity as a function of pH at higher substrate concentrations (40 mM H_2O_2 and 20 mM Br^-, respectively).

It is clear from Fig. 4*B* that at these substrate concentrations the rVCPO activity is strongly inhibited, but the reaction rates measured for the mutants are largely increased. Furthermore, the pH optima of the three mutants seem to have shifted to higher values, and strikingly, the specific activities of mutants R490A and R360A are even higher than that of the rVCPO as measured at low substrate concentrations (Fig. 4*A*). Bromoperoxidase activity of mutant H496A remained less than 0.1% that of rVCPO under all substrate concentrations measured.

The increased activities found for the mutants under high substrate concentrations may be the result of increased K_m values for H_2O_2 or Br^- or may be the combined effects of both. Furthermore, the apparently shifted pH optima of the mutants could be the result of the used fixed substrate concentrations. A more detailed steady-state analysis with the rVCPO and the three active mutant enzymes was performed in order to get more insight into the factors governing the changed kinetic.

Table I shows the kinetic parameters of these enzymes as measured for H_2O_2 and Br^- at the given pH values. The kinetic parameters were calculated from the rectangular hyperbolae that were the result of plotting the initial rates of monochlorodimedon bromination as a function of different substrate concentrations at saturating concentrations of the other substrate. Initial reaction rates were taken since the mutant enzymes showed deviations from linear reaction curves under some the conditions measured. Mutant R490A, for example, showed a rapid inactivation when measured at pH 4.2. This inactivation was especially evident at low H_2O_2 concentrations. The inactivation appeared to be the result of the low pH value since preincubation of the mutant at pH 4.2 in the absence of substrates already resulted in inactivation of the enzyme.

In line with the results reported by van Schijndel *et al.* (8) for the chlorinating activity of the native enzyme, the K_m for H_2O_2, as measured for the brominating activity of the rVCPO, was found to increase rapidly at low pH. At pH values higher than 6 the values of the K_m for H_2O_2 became too small to obtain accurate data. However, the value of the K_m for Br^- is hardly affected by pH. As has also been reported for the chlorination reaction (8), a maximal rate in the bromination is found at low pH, whereas a decrease in activity is found at higher pH values.

Inspection of Table I shows that for all mutant enzymes the K_m values for both H_2O_2 and Br^- are increased considerably. As in the rVCPO the K_m for H_2O_2 increases in value at lower pH values. However, although the K_m for Br^- of the rVCPO is not affected by pH, the mutants show an increase in this K_m at higher pH values.

As anticipated from the results depicted in Figs. 3 and 4, mutant R360A is least affected in its kinetic properties. The optimal value of k_{cat} (298–333 s^{-1}) of the bromoperoxidase reaction of this mutant is shifted approximately 2 pH units to higher pH when compared with that of the rVCPO. However, the optimal value of k_{cat} of the mutant is of similar magnitude as that of the rVCPO at pH 4.2 (230–253 s^{-1}). Mutant R490A also shows a shift in the optimum of the k_{cat} value although apparently to a less alkaline pH as the R360A mutant. Table I shows that the K_m for H_2O_2 of the R490A mutant below pH 5.5 has increased to 11.6 mM. Thus part of the sharp decline in the activity of this mutant at low pH as depicted in Fig. 4*B* results from the use of 40 mM H_2O_2. Strikingly, k_{cat} of mutant R490A is also similar to that of the rVCPO when both are compared under optimal conditions.

From the k_{cat} values it could be concluded that mutants R360A and R490A are better enzymes at high pH values than rVCPO. However, to make such a comparison the specificity constant (k_{cat}/K_m) needs also to be taken into account. Inspection of the specificity constants of rVCPO and the mutants in Table I reveals that the mutants are severely affected in catalytic activity. This is evident when we compare rVCPO to the mutant R360A which is least affected. Even at pH 4.2, where the specificity constant of R360A for Br^- has its optimum, and at pH 7 where this constant is high for H_2O_2, these values are still lower than those from the rVCPO.

The kinetic parameters are most impaired in the case of mutant K353A (Table I), and no clear pH optimum is found in the activity of this mutant. k_{cat} of this mutant is only 14% that of rVCPO when both are compared under optimal conditions.

DISCUSSION

Steady-state kinetic analysis of VHPOs has indicated that these enzymes work according to a substrate-inhibited ping

TABLE I
Kinetic parameters of rVCPO and mutants R360A, R490A, and K353A

Enzyme	pH / substrate	4.2 Km	4.2 kcat	4.2 kcat/Km	5.2 Km	5.2 kcat	5.2 kcat/Km	6.3 Km	6.3 kcat	6.3 kcat/Km	7.0 Km	7.0 kcat	7.0 kcat/Km
		μM	s^{-1}	$M^{-1}\ s^{-1}$	μM	s^{-1}	$M^{-1}\ s^{-1}$	μM	s^{-1}	$M^{-1}\ s^{-1}$	μM	s^{-1}	$M^{-1}\ s^{-1}$
rVCPO	H_2O_2	90	250	2.6×10^6	35	203	5.8×10^6	<5	33	$>6.6 \times 10^6$	<5	5	$>1.0 \times 10^6$
	Br^-	<5	253	$>5.1 \times 10^7$	9	248	2.8×10^7	7	37	5.3×10^6	10	6	6.0×10^5
R490A	H_2O_2	11,600	109	9.4×10^3	5500	351	6.4×10^4	1200	239	2.0×10^5	600	110	1.8×10^5
	Br^-	200	109	5.5×10^5	1400	357	2.6×10^5	4300	255	5.9×10^4	2500	113	4.5×10^4
R360A	H_2O_2	2500	107	4.3×10^4	1100	270	2.5×10^5	1400	298	2.1×10^5	150	115	7.7×10^5
	Br^-	38	56	1.5×10^6	300	225	7.5×10^5	700	333	4.8×10^5	1100	117	1.1×10^5
K353A	H_2O_2	12,300	24	2.0×10^3	3800	28	7.4×10^3	4400	36	8.2×10^3	1000	29	2.9×10^4
	Br^-	4500	24	5.3×10^3	4800	32	6.7×10^3	9400	36	3.8×10^3	18,600	32	1.7×10^3

Kinetic parameters were determined in sodium citrate/citric acid buffers adjusted to the desired pH and in the presence of 100 μM vanadate. Kinetic parameters for one substrate (H_2O_2 or Br^-) were determined in the presence of a concentration of 5–10 times the determined K_m of the other substrate (Br^- or H_2O_2) and were calculated using Enzyme Kinetics (version 1.4 Macintosh Trinity software) on the basis of direct linear fits using at least eight substrate concentrations varying from 0.2 to 5 times the K_m for each mutant under each condition measured.

pong bi bi mechanism (1, 6, 8, 37–39). H_2O_2 is the first substrate that binds, and it is shown that the affinity for this substrate increases with increasing pH. For the VCPO from *C. inaequalis* K_m values for H_2O_2 have been reported to vary from 0.5 mM at pH 3.2 to 10 μM at pH 5 (8). The kinetic analyses of the VHPOs indicate that binding of H_2O_2 to the enzyme is inhibited when a group with a pK_a between 5.6 and 6.5 is protonated (1, 8, 38). Vanadate-coordinated water or a histidine residue were indicated as possible active site groups with pK_a values in these ranges. Inspection of the VCPO active site revealed that His^{404} is a likely candidate for such a group (11). A H404A mutant has also been studied (35), and this mutant has lost its chlorinating activity. However, in this mutant there is a change in conformation with an effect on the active site making direct conclusions about the role of His^{404} in catalysis difficult.

The halide is the second substrate that binds to the enzyme, and the pH profile for halide binding was shown to be opposite to that of H_2O_2 binding. For the *C. inaequalis* VCPO the K_m for chloride was shown to vary from 0.25 mM at pH 4 to 116 mM at pH 8 (8). Recently, the K_m for bromide of the *C. inaequalis* enzyme was shown to be as low as 9 μM at pH 5 (36).

Fig. 5 shows a minimal catalytic mechanism for the VHPOs that is a combination and extension of such schemes published previously (1, 8, 14, 38–40) and that also takes into account the results presented in this paper. Obviously binding of vanadate is of paramount importance in any scheme describing VHPO catalysis. Since vanadate is only covalently linked to His^{496} the results obtained with the H496A mutant are not very surprising. Analysis of the H496A crystal structure very recently revealed (35) that when the crystals are soaked in the presence of 1 mM vanadate, the metal ion can still be found in the active site of the mutant. However, the covalent bond is lost, and vanadate is found in a tetrahedral conformation hydrogen-bonded to the same residues as in the rVCPO and the native enzyme indicating that the covalent bond is essential for catalytic activity.

The effects of the mutations of the equatorial residues are less dramatic and, although mutant R360A has residual VCPO activity, the basic feature of each of these mutants is that it apparently has changed into a VBPO. This becomes clear when the specificity constants of the mutants are compared with those of the VBPO of *Ascophyllum nodosum* (1). The specificity constants for Br^- have a maximal value around pH 4 and are $1.8 \cdot 10^5$, $1.5 \cdot 10^6$, and $5.5 \cdot 10^5$ $M^{-1}\ s^{-1}$ for *A. nodosum*, R360A, and R490A, respectively. The specificity constants for H_2O_2 are maximal around pH 7 and are $2.8 \cdot 10^6$, $7.7 \cdot 10^5$, and $1.8 \cdot 10^5$ $M^{-1}\ s^{-1}$ for *A. nodosum*, R360A, and R490A, respectively.

It is obvious that mutation R360A has a relatively mild effect as compared with R490A or K353A, which strongly affect the catalytic efficiency. We will describe below how the consequences of the mutations can be explained when the charge and the hydrogen-bonding network in the VCPO active site are taken into account.

The native enzyme is shown in Fig. 5*A*, the kinetic events described in *A*—*C* are identical to those proposed by Messerschmidt *et al.* (14) and lead to the side on bound peroxide as observed in the structure of the peroxide intermediate (14).

Halide binding is the next step in catalysis. Binding can occur directly at the vanadate prior to its oxidation (14) or the halide can perform a nucleophilic attack on one of the oxygens of the bound peroxide. Based on mechanistic studies with model compounds (41) and on the assumption that direct binding of the halide will decrease its nucleophilicity, we favor the latter possibility.

The basic residues Lys^{353}, Arg^{360}, and Arg^{490} compensate for the negative charges on the vanadate oxygens by forming hydrogen bonds with these atoms. Changing any of these residues into an alanine will increase the overall negative charge in the active site, which is expected to influence catalysis. Accordingly, we have shown that mutants K353A and R490A have lost the ability to oxidize chloride while also mutant R360A is severely impaired in chloride oxidation. However, these three mutants are still able to oxidize the less electronegative bromide and have thus become bromoperoxidases by definition.

It can be rationalized that the positively charged residues in the active site (together with vanadate as a Lewis acid) decrease the electron density of the bound peroxide thereby activating this substrate. The effects of the mutations in the equatorial positions are most severe for mutant K353A. The K_m values for H_2O_2 and Br^- are largely increased, and also k_{cat} is only 15% that of the rVCPO when both are compared at their optimal pH values.

In the crystal structure of the peroxide form of the enzyme (14), it can be seen that Lys^{353} is the only positively charged residue that is directly linked to the bound peroxide, via a strong hydrogen bond with peroxide oxygen OV4. This can explain the importance of this residue in catalysis since in addition to the above-mentioned general electron-withdrawing effect, this hydrogen bond (see Fig. 5, *C* and *D*) may also polarize the bound peroxide. This will make the peroxide oxygen OV2 more susceptible toward a nucleophilic attack by the halide (Fig. 5*D*) as already suggested by Hamstra *et al.* (42). Binding of the halide to the partially positive peroxide oxygen breaks the peroxide bond, and the nucleophilic OX^- group is formed (Fig. 5*D*). The OX^- group will take up a proton from an incoming water, possibly activated by His^{404} (Fig. 5*E*), and leave the coordination sphere as hypohalous acid. The formed hydroxide, resulting from the deprotonation of the water molecule, can simultaneously take the empty coordination site on

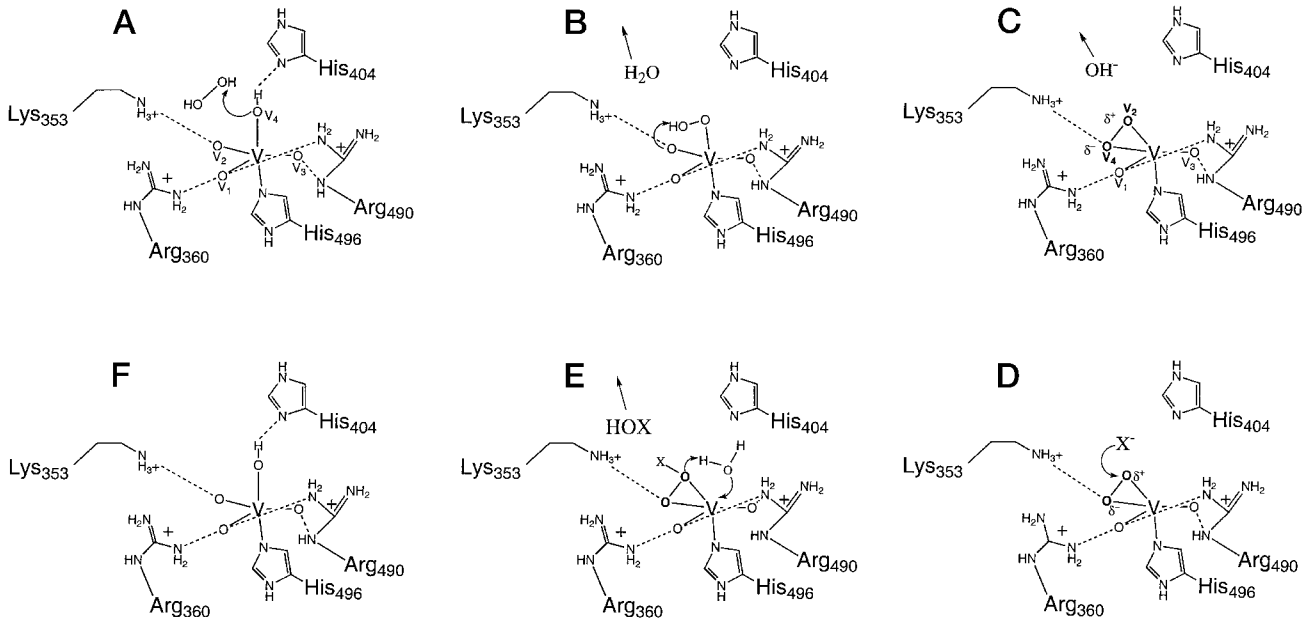

FIG. 5. **Minimal reaction scheme for VCPO catalysis.** (See text for details.)

the vanadium, and the native structure is formed back again (Fig. 5*F*).

Arg^{360} and Arg^{490} do not form hydrogen bonds with any of the oxygens of the bound peroxide, and as such the effects of the Arg^{360} or Arg^{490} to Ala mutations are expected to be less drastic than those of the Lys^{353} to Ala mutation. The increased negative charge in the active site, however, will weaken the activation of the bound peroxide. Since Arg^{360} donates one hydrogen bond only (to OV1) and Arg^{490} donates one to OV1 and one to OV3, the effects observed in the R360A mutant are expected to be milder than those observed in the R490A mutant. This is confirmed by the analysis of these mutants.

The decreased activation of this bound peroxide may also result in the 100–1000-fold increase in the K_m values for bromide as observed for the mutants. In this respect it is noteworthy that the R360A mutant, for which the K_m values for bromide are affected the least, still has residual chlorinating activity. It has been suggested (40) that the activated oxygen OV2 (Fig. 5, *C* and *D*) is protonated, thus creating a full positive charge on this atom. If one assumes that such protonation occurs in VCPO while the activated oxygen is only partially positive in the VBPOs and the mutants, one can explain both the high oxidizing ability and the relatively low value of the K_m for bromide in VCPO. Protonation of the activated oxygen may also explain the strong pH dependence of the K_m for chloride in VCPO (6), whereas the K_m for bromide in VBPO and the mutants is only slightly affected when the pH is varied (1, 39).

The observed pH shift in the optimal value of k_{cat} (Table I) upon mutation of Arg^{360} and Arg^{490} may be the consequence of the decrease in positive charge in the active site, which might affect the pK_a of the residues governing the pH dependence. However, residues that are involved in the decrease of k_{cat} as a function of pH have not been identified, and further analysis has to answer this question.

The results of the kinetic analysis of the site-directed mutants point to the importance of the activation of the bound peroxide prior to oxidation of the halide, and very recently we indicated why this activation may be less in the VBPOs as compared with the VCPOs (43). Alignment of the active site domains 1, 2, and 3 of the VCPOs, the currently known VBPOs, and the homologous acid phosphatases suggested that the most important difference between the VCPOs and the acid phosphatases on one hand and the VBPOs on the other hand might be the number of residues in domain 1 bridging the lysine and arginine, which are the counterparts of the vanadate bridging Lys^{353} and Arg^{360} of *C. inaequalis*. Only in the VBPOs are there seven instead of six bridging residues. This extra residue will result in a slightly different geometry of the active site of the VBPOs. This in turn may result in a less strong hydrogen bond between the lysine and the bound peroxide and therefore in a less positively charged and less activated peroxide that is unsusceptible to a nucleophilic attack by chloride at physiological concentrations.

This study has shown that His^{496} is essential for activity of the VCPO, and it is expected that the corresponding histidine is of equal importance for catalysis of the VBPOs and the homologous acid phosphatases, as was recently shown to be the case in glucose-6-phosphatase (44). Analysis of the mutants R490A, R360A, and K353A has revealed the importance of these side chains in compensating the negative charges of the vanadate oxygens. Furthermore the importance of the hydrogen bond between Lys^{353} and the bound peroxide was shown. The mutations in the vanadate coordinating side chains may also affect the affinity of the mutant enzyme for the cofactor, and we are currently performing experiments to investigate this. These results, together with the results of the analysis of site-directed mutants for His^{404} and Asp^{292} of which the crystal structures were recently determined (35), will hopefully deepen our understanding of the catalytic mechanism of the VCPO and the homologous enzymes.

REFERENCES

1. De Boer, E., and Wever, R. (1988) *J. Biol. Chem.* **263,** 12326–12332
2. Arber, J. M., De Boer, E., Garner, C. D., Hasnain, S. S., and Wever, R. (1989) *Biochemistry* **28,** 7968–7973
3. Wever, R., Krenn, B. E., De Boer, E., Offenberg, H., and Plat, H. (1988) *Prog. Clin. Biol. Res.* **274,** 477–493
4. Vollenbroek, E. G. M., Simons, L. H., Van Schijndel, J. W. P. M., Barnett, P., Balzar, M., Dekker, H. L., Van der Linden, C., and Wever, R. (1995) *Biochem. Soc. Trans.* **23,** 267–271
5. Plat, H., Krenn, B. E., and Wever, R. (1987) *Biochem. J.* **248,** 277–279
6. Van Schijndel, J. W. P. M., Vollenbroek, E. G. M., and Wever, R. (1993) *Biochim. Biophys. Acta* **1161,** 249–256
7. Van Schijndel, J. W. P. M., Simons, L. H., Vollenbroek, E. G. M., and Wever, R. (1993) *FEBS Lett.* **336,** 239–242
8. Van Schijndel, J. W. P. M., Barnett, P., Roelse, J., Vollenbroek, E. G. M., and Wever, R. (1994) *Eur. J. Biochem.* **225,** 151–157
9. Van Schijndel, J. W. P. M. (1994) *Structural and Functional Properties of Vanadium Chloroperoxidase from the Fungus Curvularia inaequalis*. Ph.D.

thesis, University of Amsterdam, Amsterdam
10. Simons, L. H., Barnett, P., Vollenbroek, E. G. M., Dekker, H. L., Muijsers, A. O., Messerschmidt, A., and Wever, R. (1995) *Eur. J. Biochem.* **229,** 566–574
11. Messerschmidt, A., and Wever, R. (1996) *Proc. Natl. Acad. Sci. U. S. A.* **93,** 392–396
12. Hemrika, W., Renirie, R., Dekker, H. L., Barnett, P., and Wever, R. (1997) *Proc. Natl. Acad. Sci. U. S. A.* **94,** 2145–2149
13. Barnett, P., Kruidbosch, D. L., Hemrika, W., Dekker, H. L., and Wever, R. (1997) *Biochim. Biophys. Acta* **1352,** 73–84
14. Messerschmidt, A., Prade, L., and Wever, R. (1997) *Biol. Chem.* **378,** 309–315
15. Hemrika, W., and Wever, R. (1997) *FEBS Lett.* **409,** 317–319
16. Stukey, J., and Carman, G. M. (1997) *Protein Sci.* **6,** 469–472
17. Shelly, L. L., Lei, K. J., Pan, C. J., Sakata, S. F., Ruppert, S., Schutz, G., and Chou, J. Y. (1993) *J. Biol. Chem.* **268,** 21482–21485
18. Lange, A. J., Argaud, D., El-Maghrabi, M. R., Pan, W., Maitra, S. R., and Pilkis, S. J. (1994) *Biochem. Biophys. Res. Commun.* **201,** 302–309
19. Lei, K. J., Shelly, L. L., Pan, C. J., Sidbury, J. B., and Yang Chou, J. (1993) *Science* **262,** 580–583
20. Chen, Y. T., and Burchell, A. (1995) in *The Metabolic and Molecular Bases of Inherited Disease* (Scriver, C. R., Beaudet, A. L., Sly, W. S., Valle, D., Stanburry, J. B., Wyngaarden, J. B., and Frederickson, D. S., eds) Vol. 7, pp. 935–965, McGraw-Hill Inc., New York
21. Kanoh, H., Kai, M., and Wada, I. (1997) *Biochim. Biophys. Acta* **1348,** 56–62
22. Carman, G. M. (1997) *Biochim. Biophys. Acta* **1348,** 45–55
23. Brindley, D. N., and Waggoner, D. W. (1998) *J. Biol. Chem.* **273,** 24281–24284
24. Barnett, P. (1997) *The Fungal Vanadium Chloroperoxidase: from Primary Structure to Function.* Ph.D. thesis, University of Amsterdam, Amsterdam
25. Klebe, R. J., Harries, J. V., Sharp, D., and Lacroute, F. (1980) *Gene* (*Amst.*) **11,** 11–19
26. St. John, T. P., and Davis, R. W. (1981) *J. Mol. Biol.* **152,** 285–315
27. Johnston, M., and Davis, R. W. (1984) *Mol. Cell. Biol.* **4,** 1440–1448
28. Gietz, R. D., and Sugind, A. (1988) *Gene* (*Amst.*) **74,** 527–534
29. Laemmli, U. K. (1970) *Nature* **227,** 680–685
30. Bradford, M. M. (1976) *Anal. Biochem.* **72,** 248–254
31. Sambrook, J., Fritsch, E. F., and Maniatis, T. (1989) *Molecular Cloning: A Laboratory Manual*, Cold Spring Harbor Laboratory, Cold Spring Harbor, NY
32. Brake, A. J. (1989) *Bio/Technology* **13,** 269–280
33. De Boer, E., Tromp, M. G. M., Plat, H., Krenn, G. E., and Wever, R. (1986) *Biochim. Biophys. Acta* **872,** 104–115
34. De Boer, E., Plat, H., Tromp, M. G. M., Franssen, M. C. R., van der Plas, H. C., Meijer, E. M., Schoemaker, H. E., and Wever, R. (1987) *Biotechnol. Bioeng.* **30,** 607–610
35. Macedo-Ribeiro, S., Hemrika, W., Renirie, R., Wever, R., and Messerschmidt, A. (1999) *J. Biol. Inorg. Chem.* **4,** 209–219
36. Barnett, P., Hemrika, W., Dekker, H. L., Muijsers, A. O., Renirie, R., and Wever, R. (1998) *J. Biol. Chem.* **273,** 23381–23387
37. Soedjak, H. S., and Butler, A. (1990) *Biochemistry* **29,** 7974–7981
38. Soedjak, H. S., and Butler, A. (1991) *Biochim. Biophys. Acta* **1079,** 1–7
39. Everett, R. R., Soedjak, H. S., and Butler, A. (1990) *J. Biol. Chem.* **265,** 15671–15679
40. Slebodnick, C., Hamstra, B. J., and Pecoraro, V. L. (1997) in *Metal Sites in Proteins and Models* (Sadler, P. J., ed) Vol. 89, pp. 51–108, Springer-Verlag, Berlin
41. Butler, A., and Baldwin, A. H. (1997) in *Metal Sites in Proteins and Models* (Sadler, P. J., ed) Vol. 89, pp. 109–132, Springer-Verlag, Berlin
42. Hamstra, B. J., Colpas, G. J., and Pecoraro, V. L. (1998) *Inorg. Chem.* **37,** 949–955
43. Hemrika, W., Renirie, R., Dekker, H., and Wever, R. (1998) in *Vanadium Compounds: Chemistry, Biochemistry, and therapeutic Applications* (Tracey, A. S., and Crans, D. C., eds) pp. 186–201, Oxford University Press, Washington, D. C.
44. Pan, C.-J., Lei, K.-J., Annabi, B., Hemrika, W., and Chou, J. Y. (1998) *J. Biol. Chem.* **273,** 6144–6148
45. Guex, N., and Peitsch, M. C. (1997) *Electrophoresis* **18,** 2714–2723